Journal of Analytical Science and Technology
a SpringerOpen Journal

RESEARCH Open Access

NMR studies of a Glutaredoxin 2 from Clostridium oremlandii

Eun Hye Lee[1,2], Hae-Kap Cheong[1] and Hye-Yeon Kim[1*]

Abstract

Background: Grx2 is a glutaredoxin from gram positive bacterium *Clostridium oremlandii* (strain OhILAs), which is Cys-homolog of selenoprotein Grx1. Grx2 is a poor reductant of selenoprotein MsrA not like Grx1 while the reducing activity is reversed in two Grxs for Cys version of MsrA.

Methods: The wild-type Grx2 and the C15S mutant were overexpressed in *E.coli* and purified by affinity chromathography and gel filtration. The 3D NMR spectra was collected and assigned all the backbone chemical shifts including Cα, Cβ, CO, HN, and N of Grx2 and C15S mutant. The protein folding of two proteins were evaluated by circular dichroism.

Results: Here we report the protein purification and NMR spectroscopic study of recombinant Grx2 and the C15S mutant. The HSQC spectrum of two proteins show chemical shift difference for residues 8-19, 52-55,66. The circular dichroism result shows that recombinant proteins are well folded.

Conclusion: The conformation of two proteins resembles the oxidized form (wild-type Grx2) and the reduced form (the C15S mutant). The residues showing chemical shift difference will join the conformational change of Grx2 upon a disulfide formation.

Keywords: Grx2, MsrA, *Clostridium oremlandii*, Backbone assignment, NMR

Introduction

Glutaredoxins (Grxs) have been studied in decades and described as glutathionine-dependent reductases of the disulfide formed during its catalytic cycle (Holmgren et al. 2005). Grxs are able to restore the growth of *E.coli* in a mutant lacking thioredoxin (Trx) (Holmgren 1976). Trxs and Grxs share several functions but Grxs are more versatile in choice of substrate and reaction mechanisms (Holmgren 1989). Two groups of Grxs, dithiol and monothiol Grxs, are divided upon catalytic site and functional mechanism (Lillig et al. 2008). Dithiol Grxs contain the characteristic CPYC active site motif and monothiol Grxs lack the C-terminal active site cysteine in the CGFS motif. Both Grxs utilize glutathionine (GSH) as a substrate and share structural elements of binding GSH. GSH is a major biological compound and has a pivotal role in cellular redox homeostasis (Meister 1994). The ratio of GSH and the oxidized form of GSH, glutathionine disulfide (GSSG), are major determinants of cellular redox state. Grxs could regulate the cellular processes related with the GSH-GSSG redox state. Many organisms contain a unique composition of Grxs. *E.coli* contains four Grxs, two classical dithiol Grxs (Grx1 and Grx3), one unusual dithiol Grx (Grx2), and one monothiol Grx (Grx4) (Vlamis-Gardikas & Holmgren 2002; Fernandes & Holmgren 2004). The structures of Grxs have been studied by X-ray crystallography and NMR spectroscopy. Grxs belong to the Trx fold family which consists of a four stranded β-sheet surrounded by three α-helices. In addition to the active site motif, two additional regions are present for binding of GSH; the residues preceding the *cis*-proline (consensus: TVP) and the residues following the GG-motif (consensus: GGxdD) (Lillig et al. 2008).

Clostridium oremlandii (strain OhILAs) is a selenoprotein-rich organism and contains selenoprotein MsrA and selenoprotein Grx1 (Kim et al. 2006). *C.oremlandii* has a Cys-homolog protein of selenoprotein Grx1 which is defined as glutaredoxin 2 (Grx2). MsrA catalyzes the

* Correspondence: hyeyeon@kbsi.re.kr
[1]Division of Magnetic Resonance Research, Korea Basic Science Institute, Ochang, Chungbuk, Korea
Full list of author information is available at the end of the article

reduction of oxidized methionine residue in cellular proteins. A cysteine residue at the active site of MsrA is oxidized after the catalysis and then recycled by reductases like Trx. Selenoprotein MsrA shows 20-fold higher catalytic activity than its Cys-containing form instead of selenocysteine (Sec). This organism uses Grx proteins, Grx1 or Grx2, for reduction of the oxidized MsrA instead of Trxs. Selenoprotein Grx1 is a strong reductant of selenoprotein MsrA while Grx2 shows poor reducing activity for selenoprotein MsrA (Boschi-Muller et al. 2000). Although Grx1 and Grx2 share sequence homology of 55%, the reducing activity for selenoprotein MsrA is extremely different. Interestingly, the reducing activity of Grxs is reversed between Cys vesion of Grx1 and wild-type Grx2 for Cys version of MsrA. Grx2 shows high reducing activity whereas Cys version Grx1 shows almost no activity in reduction of Cys version of MsrA (Kim et al. 2011). Previously, we reported the backbone assignment result of Cys version Grx1 (Lee et al. 2012). To investigate the structural characteristics of Grx2, we have performed the NMR spectroscopy of Grx2 and its C15S mutant. Grx2 consists of 85 amino acid residues including three cysteine residues in its sequence and contains a conserved CGPC motif of dithiol Grxs. Two cysteine residues are defined as catalytic and resolving cysteines depending on the role during the cataylsis. Catalytic cysteine reduces the substrate and then the oxidized cysteine is recovered by the resolving cysteine. The resolving cysteine C15 is introduced to obtain the advantages in monitoring the molecular interaction between catalytic cysteines of Grx2 and MsrA. The wild-type and the C15S mutant of Grx2 are subjected to NMR experiments and circular dichroism. Here, we report purification and NMR backbone assignment of recombinant Grx2 proteins.

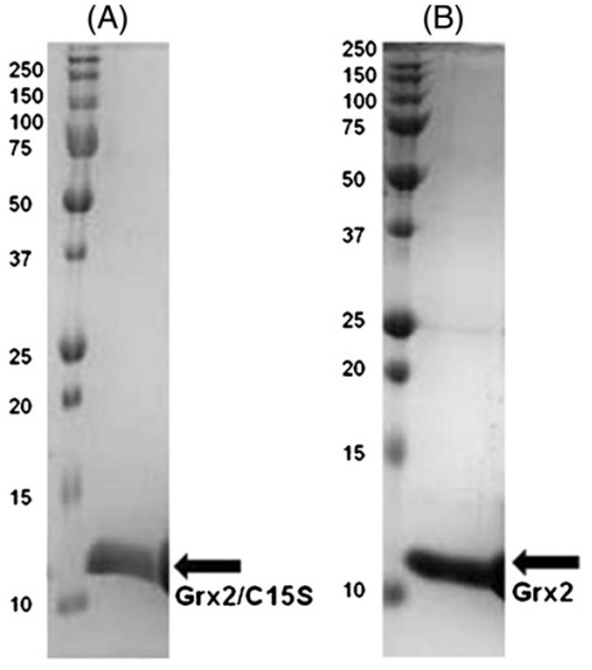

Figure 1 Protein purification. Samples from all purification steps were confirmed by the SDS-PAGE analysis. The expressed Grx2 proteins were purified using the HisTrap column and then applied to the Superdex 75 gel chromatography column. The purified C15S mutant (**A**) and wild-type Grx2 (**B**) proteins show >98% purity. The migration of the molecular mass markers is indicated on the left.

Methods

Cloning, expression and purification

Grx2 (residues 1–85) from genomic DNA of *Clostridium oremlandii* was cloned into the expression vector pET21b (Novagen). The recombinant plasmids were transformed to *E.coli* BL21(DE3) cells for protein overexpression. The wild-type Grx2 and the C15S mutant of Grx2 (the C15S mutant) were expressed with the C-terminal Histag (LEHHHHHH). The cells were grown in M9 minimal media containing 100 μg/ml ampicilin for $^{13}C/^{15}N$ double labeling at 37°C until OD_{600} reached 0.6. Then protein overexpression was induced by addition of 0.5 mM IPTG at 18°C for 20 h. The cells was harvested by centrifugation at 4,500 rpm for 20 min and resuspended in the ice-cold buffer A (20 mM Tris–HCl, pH 7.5, 300 mM NaCl, 4 mM $MgCl_2$). Harvested cells were disrupted by sonication and centrifuged at 13,000 rpm for 50 min at 4°C. The supernatant was loaded onto HisTrap column (GE Healthcare) equilibrated with buffer A and recombinant protein was eluted by gradient increasing of imidazole concentration. The protein was concentrated to ~2 ml and applied to HiLoad 16/60 Superdex-75 (GE healthcare) equilibrated with 20 mM HEPES, pH 7.0, 100 mM NaCl. The eluted protein was concentrated to 1 mM for NMR study.

NMR data acquisition and analysis

NMR experiments were performed at 25°C using 1 mM of $^{13}C,^{15}N$-labeled Grx2 and the C15S mutant samples in 20 mM HEPES, pH 7.0, 100 mM NaCl. 10% D_2O of total sample volume and 5 mM DTT were added to both samples before experiments. NMR data were collected by Bruker Avance 800-MHz NMR spectrometer (Korea Basic Science Institute, Korea) for three days. The backbone chemical shift were obtained by three-dimensional heteronuclear correlation experiments: HNCO, HN(CA)CO, HNCA, HN(CO)CA, HNCACB, CBCA(CO)NH (Wishart et al. 1995). NMR experiments of Grx2 including three spectra, HSQC, HNCACB and CBCA(CO)NH, were performed at same condition. All NMR data were processed and analyzed by TopSpin (Bruker BioSpin), NMRPipe (Delaglio et al. 1995) and then applied to AutoAssign server (Zimmerman et al. 1997) and further

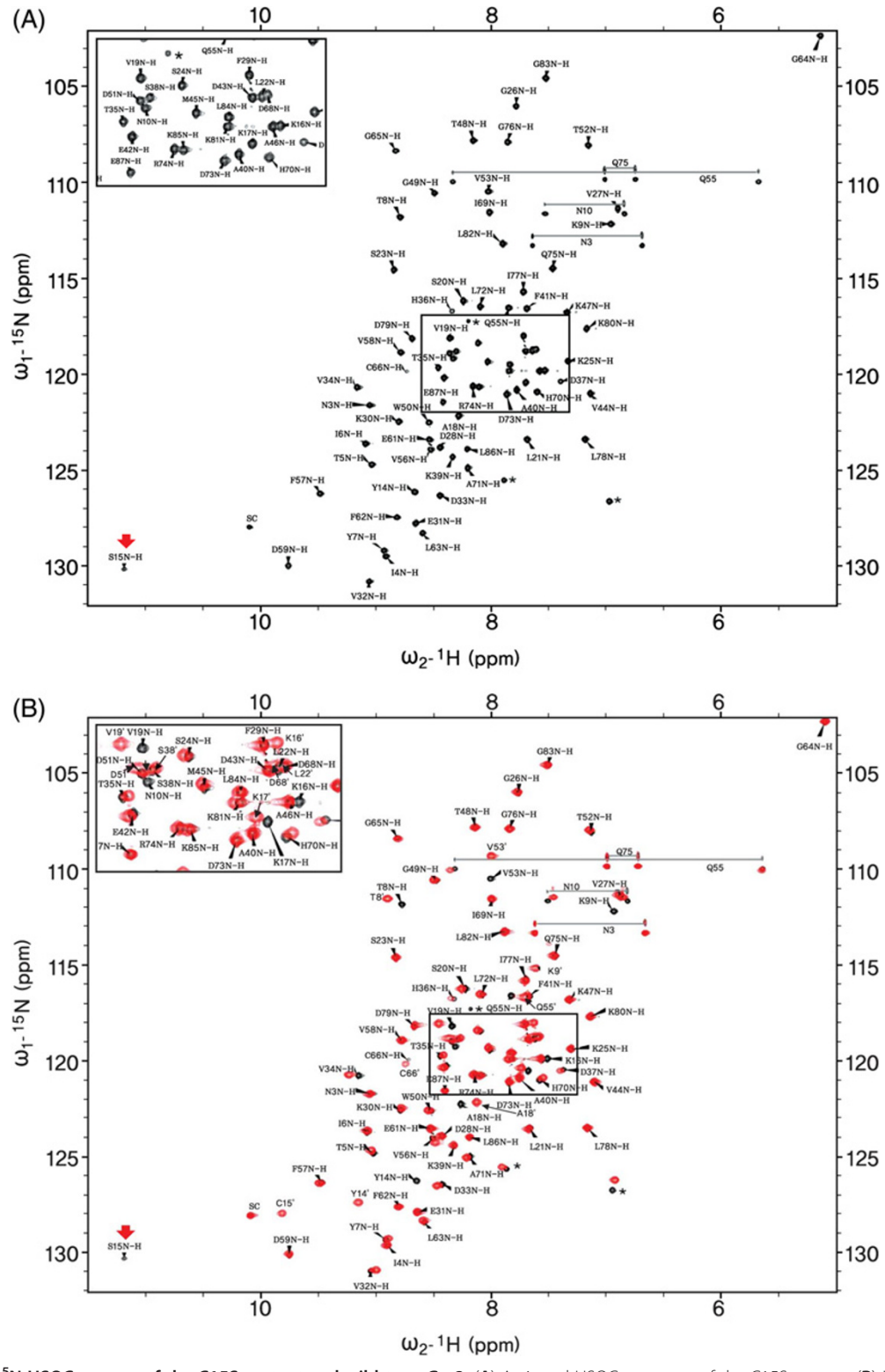

Figure 2 ^{1}H-^{15}N HSQC spectra of the C15S mutant and wild-type Grx2. (**A**) Assigned HSQC spectrum of the C15S mutant. (**B**) HSQC spectra overlay of the C15S mutant (black) and wild-type Grx2 (red). Several residues of wild-type Grx2 protein are represented with prime(') marks. All assigned residues are labeled and one crowded region is magnified (insets). The mutated residue C15S is indicated by red arrow. The assigned set of cross peaks from amide side-chains of Asn and Gln residues is indicated using a gray horizontal bar. The unassigned peaks are marked by '*' and the tryptophan side chain is marked by 'sc'.

Table 1 Assigned backbone chemical shifts (1HN, 15 N, 13CO, 13Cα and 13Cβ) of the C15S mutant

AA	HN	N	Cα	Cβ	CO	AA	HN	N	Cα	Cβ	CO
K2	-	-	53.11	31.01	172.9	A46	7.573	119.8	51.64	15.38	176.3
N3	9.051	121.6	50.24	36.27	171.9	K47	7.341	116.7	55.65	30.68	175.9
I4	8.905	129.5	58.24	36.53	172.6	T48	8.153	107.8	59.14	68.14	173.8
T5	9.033	124.7	58.69	68.94	169.6	G49	8.49	110.5	42.89	-	171.7
I6	9.087	123.6	55.28	39.13	169.5	W50	8.535	122.5	53.42	27.5	172.8
Y7	8.926	129.2	54.69	36.8	173.5	D51	8.356	118.9	49.69	38.2	173.4
T8	8.784	111.8	57.11	69.57	170.6	T52	7.153	108	57.08	68.83	170.9
K9	6.958	112.2	52.91	34.43	175.1	V53	8.021	110.5	55.83	30.89	170
N10	8.323	119.2	52.42	35.54	172.7	P54	-	-	59.2	33.52	173.8
P13	-	-	61.69	29.38	176.9	Q55	7.844	116.5	54.31	31	172
Y14	8.659	126.1	58.27	35.19	176.2	V56	8.518	123.9	59.31	30.42	170.6
S15	11.18	130.2	61.41	51.86	172.3	F57	9.482	126.2	53.6	40.89	172.5
K16	7.612	120.4	56.83	29.69	176.5	V58	8.779	118.8	58.27	30.67	173.3
K17	7.694	120.4	56.84	30.24	176.4	D59	9.754	130	54.44	36.77	173.1
A18	8.277	122.1	52.92	16.91	175.6	E60	-	-	54.66	26.15	172.9
V19	8.354	118.1	64.72	28.92	175.6	E61	8.533	123.4	53.16	28.25	172.4
S20	8.237	116.1	59.22	59.93	174.3	F62	8.81	127.5	52.56	36.32	172.9
L21	7.68	123.4	55.33	37.92	177.2	L63	8.59	128.3	51.63	40.3	172.3
L22	7.636	118.8	55.57	37.86	176.6	G64	5.136	102.3	41.28	41.28	169.3
S23	8.838	114.5	59.36	60.24	175.3	G65	8.823	108.3	40.98	41.03	171.3
S24	8.109	118.4	58.38	60.28	172.7	C66	8.721	119.9	60.96	35.07	-
K25	7.329	119.3	52.69	30.37	174.8	D67	-	-	55.04	36.66	176.3
G26	7.779	106	43.67	-	171.7	D68	7.602	118.7	54.92	38.57	176.4
V27	7.012	112	56.67	30.7	172.2	I69	8.009	111.5	62.98	35.16	175.1
D28	8.438	123.8	51.44	38.58	173.1	H70	7.594	120.9	59.86	25.44	175
F29	7.711	118	52.92	39.09	169.9	A71	8.196	124.9	52.91	14.83	178
K30	8.796	122.4	51.96	31.66	171.5	L72	8.091	116.4	54.66	39.86	177.1
E31	8.648	127.8	51.43	28.48	173	D73	7.863	121	54.4	39.05	177
V32	9.056	130.8	58.79	29.63	171.2	R74	8.153	120.6	56.52	27.33	175.8
D33	8.44	126.3	50.56	38.56	176	Q75	7.462	114.5	53.4	27.95	173.6
V34	9.159	120.7	58.59	28.05	173.5	G76	7.854	107.9	42.97	-	172.2
T35	8.458	119.7	64.95	66.01	172.4	I77	7.713	115.7	58.9	36.87	174
H36	8.335	116.7	52.67	28.19	172.2	L78	7.18	123.4	55.31	37.16	175.1
D37	7.393	120.4	49.88	37.87	172.1	D79	8.68	118.1	55.5	37.08	175.5
S38	8.297	118.8	58.21	60.13	174.5	K80	7.165	117.6	56.33	29.42	177.8
K39	8.33	124.3	56.29	28.85	176	K81	7.843	119.8	55.12	29.3	175.3
A40	7.775	120.8	51.76	15.74	178.1	L82	7.896	113.1	52.22	39.01	173.2
F41	7.683	116.6	56.17	36.15	174.1	G83	7.521	104.5	42.96	-	171.8
E42	8.404	120.2	57.2	26.4	176.8	L84	7.835	119.5	52.36	39.76	173.9
D43	7.692	118.8	54.38	37.61	175.6	K85	8.096	120.6	52.74	30.37	173
V44	7.135	121	63.45	28.52	174.6	L86	8.2	123.9	52.29	39.69	174.5
M45	8.028	119.4	56.38	30.65	177	E87	8.413	121.4	53.69	27.68	173.3

Table 2 Assigned backbone chemical shifts (1HN, 15 N, 13Cα and 13Cβ) of Grx2

AA	HN	N	Cα	Cβ	AA	HN	N	Cα	Cβ
K2	-	-	53.23	31.02	A46	7.585	119.8	51.66	15.39
N3	9.061	121.6	50.28	36.4	K47	7.343	116.7	55.71	30.68
I4	8.912	129.5	58.31	36.49	T48	8.155	107.8	59.24	68.11
T5	9.047	124.5	63.84	-	G49	8.507	110.5	42.94	-
I6	9.084	123.5	55.37	39.11	W50	8.558	122.5	53.47	27.49
Y7	8.903	129.2	54.97	36.88	D51	8.375	118.7	49.65	38.21
T8	8.907	111.5	56.84	69.69	T52	7.168	108	57.09	68.89
K9	7.542	114.8	52.83	34.3	V53	8.015	109.4	55.83	30.74
N10	8.344	118.8	52.17	35.64	P54	-	-	59.17	33.67
P13	-	-	61.83	29.48	Q55	7.721	116.6	54.55	30.74
Y14	9.096	127.1	58.64	34.98	V56	8.494	124.1	59.31	30.37
C15	9.988	128.1	62.55	25.84	F57	9.494	126.2	53.62	40.9
K16	7.625	118.2	56.97	29.52	V58	8.79	118.8	58.31	30.64
K17	7.752	120.3	56.91	30.23	D59	9.758	129.9	54.55	36.8
A18	8.143	122.1	53	16.86	E60	-	-	54.74	26.25
V19	8.465	118	64.75	28.91	E61	8.54	123.4	53.27	28.24
S20	8.269	116.1	60	59.79	F62	8.814	127.5	52.62	36.31
L21	7.687	123.4	55.41	37.91	L63	8.601	128.1	51.66	40.33
L22	7.6	118.7	55.69	37.85	G64	5.129	102.3	41.37	-
S23	8.838	114.6	59.33	60.05	G65	8.818	108.4	41.08	-
S24	8.136	118.3	58.39	60.29	C66	8.751	120	61.06	24.51
K25	7.326	119.3	52.77	30.38	D67	-	-	55.07	36.64
G26	7.786	106	43.72	-	D68	7.63	118.6	54.99	38.61
V27	6.905	111.3	56.66	30.72	I69	8.015	111.5	62.95	35.16
D28	8.442	123.8	51.56	38.57	H70	7.563	120.8	59.94	25.43
F29	7.726	118	52.98	39.14	A71	8.227	124.9	53.03	14.85
K30	8.791	122.4	51.98	31.75	L72	8.113	116.4	54.73	39.76
E31	8.652	127.8	51.55	28.36	D73	7.856	121	54.46	39.09
V32	9.006	130.8	58.84	29.69	R74	8.169	120.6	56.53	27.34
D33	8.479	126.3	50.68	38.67	Q75	7.475	114.4	53.47	27.94
V34	9.243	120.6	58.56	28.09	G76	7.856	107.9	43.01	-
T35	8.424	119.6	64.91	65.99	I77	7.719	115.8	58.92	36.85
H36	8.36	116.7	52.76	28	L78	7.188	123.4	55.39	37.1
D37	7.419	120.4	49.91	37.86	D79	8.676	118.1	55.6	37.11
S38	8.28	118.7	58.31	60.15	K80	7.157	117.6	56.29	29.4
K39	8.338	124.3	56.3	28.85	K81	7.865	119.8	55.23	29.29
A40	7.771	120.8	51.83	15.75	L82	7.9	113.2	52.3	38.96
F41	7.7	116.5	56.24	36.16	G83	7.53	104.6	43.01	-
E42	8.425	120.2	57.29	26.38	L84	7.841	119.5	52.41	39.72
D43	7.678	118.8	54.45	37.61	K85	8.116	120.7	52.85	30.36
V44	7.118	121	63.5	28.54	L86	8.2	123.9	52.35	39.69
M45	8.04	119.2	56.4	30.71	E87	8.412	121.5	53.73	27.68

backbone assignment was performed by Sparky (Goddard & Kneller 2004) software packages.

CD analysis

CD spectra (190–250 nm) were measured at 25°C on a Jasco J-715 apparatus, using a 1.0 mm path length quartz cell. Recombinant proteins were diluted 20 times with water at a protein concentration of 50 μM. The buffer contained 1 mM HEPES, pH 7.0, 5 mM NaCl. The averaged blank spectra were subtracted.

Results and discussion

Sample preparation

The C-terminal Histag fused Grx2 and the C15S mutant proteins were overexpressed in *E.coli* BL21(DE3). The recombinant proteins were purified by nickel affinity chromatography (HisTrap column) and then applied to size-exclusion column (HiLoad 16/60 Superdex-75 column). The purified protein contained the C-terminal histag which was not removed by further treatment. Through gel filtration, Grx2 protein was eluted at a protein size of 10 kD and it means that Grx2 present as a monomer in solution. The eluted protein showed >98% purity at SDS-PAGE and concentrated to 1 mM for NMR measurements. The final purified proteins are shown in Figure 1.

Backbone assignment

The HSQC spectrum of the C15S mutant shows doublet peaks generated by intermolecular disulfide bond in oxidative condition. The doublet peaks disappear after addtion of DTT to the sample at concentration of 5 mM. We have assigned 92% of the expected backbone ^{1}H-^{15}N correlations (77 out of 83; Grx2 contains 2 proline residues) and 96% of all ^{13}CO, $^{13}C\alpha$ and $^{13}C\beta$ (239 out of 249; Figure 2). The six residues, M1, K2, Y11, C12, E60 and D67, are not visible in HSQC spectrum. The two residues of C-terminal histag (86LEHHHHHH93) were assigned the backbone chemical shifts (Figure 2A). In HSQC spectrum, three ^{1}H-^{15}N correlations are unassigned which lost their conectivity between assigned residues. The assigned chemical shifts (Cα, Cβ, CO, HN, and N) of the C15S mutant were summarized in Table 1. NH_2 group of Asn and Gln side-chains generally produce two split HSQC cross peaks that were identified in the measured HSQC spectrum. All possible 4 set of amide side-chains peaks were identified in the HSQC spectrum. Residues N3, N10, Q55 and Q75 made two split HSQC cross peaks which are indicated by gray line between two peaks. There is one tryptophan residue in Grx2 protein and the side chain NH resonance of W50 residue was assigned in HSQC spectrum. The missing residues in HSQC spectrum are expected to be partially solvent-exposed or have possible conformational

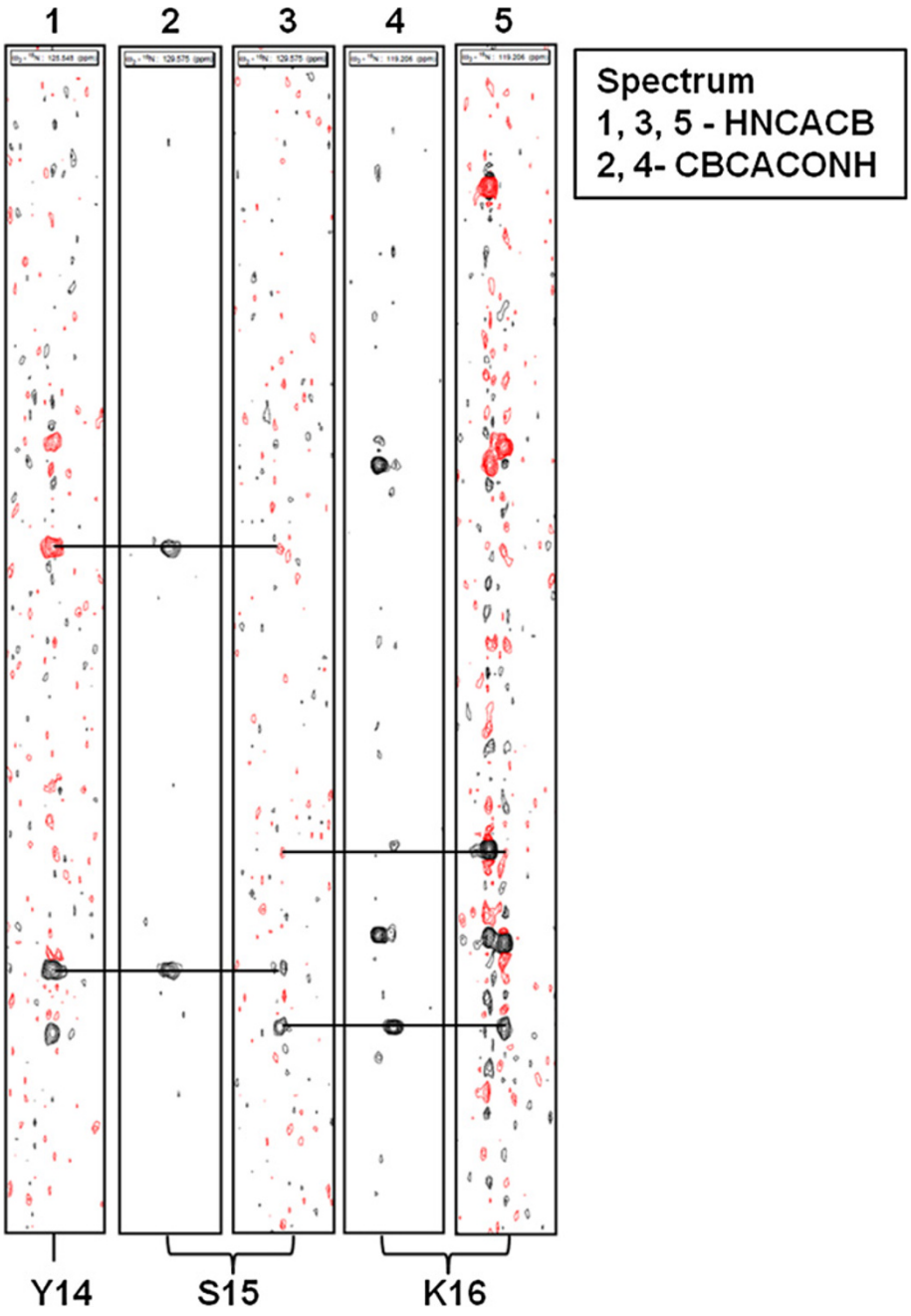

Figure 3 The strip plot of S15 residue in the C15S mutant using spectra of HNCACB and CBCACONH. The sequential connectivity is observed in neighboring residues Y14, S15 and K16 except 13Cβ of S15 showing low intensity. The peaks are colored by black (positive peak) and red (negative peak).

exchange within NMR time scale. The unassigned three peaks may originated from the remained hexahistidine tag. The ^{1}H-^{15}N correlations of Grx2 are assigned on HSQC spectrum based on the C15S mutant assignments and HSQC spectra of two proteins are superposed (Figure 2B). Some ambigouos peaks are assigned by additional experiments of HNCACB, CBCA(CO)NH using ^{13}C,^{15} N-labeled Grx2. The assigned chemical shifts (Cα, Cβ, HN, and N) of Grx2 were summarized in Table 2. The ^{1}H-^{15} N correlations of Grx2 are assigned execept two correlations which are remained in unassigned in the C15S mutant spectrum. In HSQC spectrum of Grx2, ^{1}H-^{15} N correlations of 77 residues are shown and they are common residues in the C15S mutant. Most residues are represented at the identical position of HSQC spectrum while some residues show large chemical shift

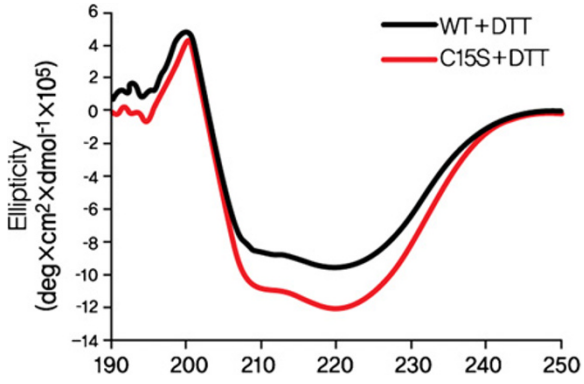

Figure 4 The circular dichroism results for recombinant proteins. The CD spectra at 50 μM Grx2 proteins were obtained in 1 mM HEPES at pH 7.0 and 5 mM NaCl at 25℃. The values are expressed as mean residue molar ellipticity (θ) in deg cm^2 $dmol^{-1}$.

change between wild-type Grx2 and the C15S mutant. The chemical shift of S15 residue has extremely high ^1H chemical shift of 11.1 ppm than 9.8 ppm of C15 residue. The 11.1 ppm can be observed in serine residue which has 1H chemical shift range of 3.76 ppm 12.33 ppm according to Biological Magnetic Resonance data Bank. The magnitude of the chemical shift depends upon the type of nucleus and the details of the electron motion in the nearby atoms and molecules (Hobbie 1998). The >1 ppm chemical shift difference may caused by extensive alteration of circumstance near proton in amino group of S15 residue. The strip plot of S15 residue with adjacent residues are represented in Figure 3. The residues K9, Y14 and C15 have chemical shift difference over 0.5 ppm and T8, K16, A18, V19, V53, Q55 and C66 residues have over 0.1 ppm. These residues could be grouped to three regions, residues 8–19 including C15 residue, residues 52TVPQ55, and residue C66. The substitution of resolving cysteine to serine may induce the conformational change near active site that is related to oxidation state of Grx2. However, there is a possibility that the chemical shift difference is occurred by the simple change of chemical environments near C15 or S15 residue without no structural change. In addition, two Grx2 proteins have well-folded structure which are validated by circular dichroism (Figure 4).

Conclusions

The substitution of resolving cysteine to serine occured conformational change and these residues may be related to oxidation state of Grx2. Two proteins show different HSQC spectrum even in the reduced condition made by DTT addition. The addition of 5 mM DTT was not enough to break the intramolecular disulfide bond but the intermolecular disulfide bond. The resolviong C15 residue makes intramolecular disulfide bond with catalytic C12 residue in wild-type Grx2. Wild-type Grx2 keeps two cysteine residues which can form a disulfide bond while the C15S mutant keeps one cysteine residue and is not able to form it. The conformation of two proteins resembles the oxidized form (wild-type Grx2) and the reduced form (the C15S mutant). The residues showing chemical shift difference will join the conformational change of Grx2 upon a disulfide formation. These results will be useful to the structural study of oxidized and reduced Grx2 and the interaction study with MsrA

Competing interests

The authors declare that they have no competing interests.

Authors' contributions

EHL carried out the smaple preparation, NMR studies and circular dichroism analysis. EHL, HKJ. and H-YK. drafted the manuscript. All authors read and approved the final manuscript.

Acknowledgements

This work was supported by the NMR research program of Korea Basic Science Institute to H.-Y.K. We thank Kim Hwa-Young (Yeungnam University) for providing the Grx2 constructs.

Author details

[1]Division of Magnetic Resonance Research, Korea Basic Science Institute, Ochang, Chungbuk, Korea. [2]Division of Biotechnology, College of Life Sciences and Biotechnology, Korea University, Seoul, Korea.

Received: 13 March 2013 Accepted: 13 March 2013
Published: 18 April 2013

References

Boschi-Muller S, Azza S, Sanglier-Cianferani S, Talfournier F, Van Dorsselear A, Branlant G (2000) A sulfenic acid enzyme intermediate is involved in the catalytic mechanism of peptide methionine sulfoxide reductase from Escherichia coli. J Biol Chem 275:35908–35913

Delaglio F, Grzesiek S, Vuister GW, Zhu G, Pfeifer J, Bax A (1995) NMRPipe: a multidimensional spectral processing system based on UNIX pipes. J Biomol NMR 6:277–293

Fernandes AP, Holmgren A (2004) Glutaredoxins: glutathione-dependent redox enzymes with functions far beyond a simple thioredoxin backup system. Antioxid Redox Signal 6:63–74

Goddard TD, Kneller DG (2004) SPARKY 3. University of California, San Francisco

Hobbie RK (1998) Intermediate Physics for Medicine and Biology. 2nd Ed. Wiley

Holmgren A (1976) Hydrogen donor system for *Escherichia coli* ribonucleoside-diphosphate reductase dependent upon glutathione. Proc Natl Acad Sci U S A 73:2275–2279

Holmgren A (1989) Thioredoxin and glutaredoxin systems. J Biol Chem 264:13963–13966

Holmgren A, Johansson C, Berndt C, Lonn ME, Hudemann C, Lillig CH (2005) Thiol redox control via thioredoxin and glutaredoxin systems. Biochem Soc Trans 33:1375–1377

Kim HY, Fomenko DE, Yoon YE, Gladyshev VN (2006) Catalytic advantages provided by selenocysteine in methionine-S-sulfoxide reductases. Biochemistry 45:13697–13704

Kim MJ, Lee BC, Jeong J, Lee KJ, Hwang KY, Gladyshev VN, Kim HY (2011) Tandem use of selenocysteine: adaptation of a selenoprotein glutaredoxin for reduction of selenoprotein methionine sulfoxide reductase. Mol Microbiol 79:1194–1203

Lee EH, Kim EH, Kin HY, Hwang KY, Kim HY (2012) NMR spectroscopic study of a Glutaredoxin1 from *Clostridium oremlandii*. JAST 3:154–159

Lillig CH, Berndt C, Holmgren A (2008) Glutaredoxin systems. Biochim Biophys Acta 1780:1304–1317

Meister A (1994) Glutathione-ascorbic acid antioxidant system in animals. J Biol Chem 269:9397–9400

Vlamis-Gardikas A, Holmgren A (2002) Thioredoxin and glutaredoxin isoforms. Methods Enzymol 347:286–296
Wishart DS, Bigam CG, Yao J, Abildgaard F, Dyson HJ, Oldfield E, Markley JL, Sykes BD (1995) 1H, 13C and 15N Chemical Shift Referencing in Biomolecular NMR. J Biomol NMR 6:135–140
Zimmerman DE, Kulikowski CA, Feng W, Tashiro M, Chien C-Y, Ríos CB, Moy FJ, Powers R, Montelione GT (1997) Artificial intelligence methods for automated analysis of protein resonance assignments. J Mol Biol 269:592–610

doi:10.1186/2093-3371-4-2
Cite this article as: Lee *et al.*: **NMR studies of a Glutaredoxin 2 from Clostridium oremlandii.** *Journal of Analytical Science and Technology* 2013 **4**:2.